ARTICLE

TGFβ modulates cell-to-cell communication in early epithelial-to-mesenchymal transition

**C. E. Hills · E. Siamantouras · S. W. Smith ·
P. Cockwell · K.-K. Liu · P. E. Squires**

Abstract

Aims/hypothesis A key pathology in diabetic nephropathy is tubulointerstitial fibrosis. The condition is characterised by increased deposition of the extracellular matrix, fibrotic scar formation and declining renal function, with the prosclerotic cytokine TGF-β1 mediating many of these catastrophic changes. Here we investigated whether TGF-β1-induced epithelial-to-mesenchymal transition (EMT) plays a role in alterations in cell adhesion, cell coupling and cell communication in the human renal proximal tubule.

Methods Whole-cell and cell compartment abundance of E-cadherin, N-cadherin, snail, vimentin, β-catenin and connexin-43 was determined in human kidney cell line (HK)2 and human proximal tubule cells with or without TGF-β1, using western blotting and immunocytochemistry, followed by quantification by densitometry. The contribution of connexin-43 in proximal tubule cell communication was quantified using small interfering

RNA knockdown, while dye-transfer was used to assess gap junctional intercellular communication (GJIC). Functional tethering was assessed by single-cell force spectroscopy with or without TGF-β1, or by immuno-neutralisation of cadherin ligation.

Results High glucose (25 mmol/l) increased the secretion of TGF-β1 from HK2 cells. Analysis confirmed early TGF-β1-induced morphological and phenotypical changes of EMT, with altered levels of adhesion and adherens junction proteins. These changes correlated with impaired cell adhesion and decreased tethering between coupled cells. Impaired E-cadherin-mediated adhesion reduced connexin-43 production and GJIC, these effects being mimicked by neutralisation of E-cadherin ligation. Upregulation of N-cadherin failed to restore adhesion or connexin-43-mediated GJIC.

Conclusions/interpretation We provide compelling evidence that TGF-β1-induced EMT instigates a loss of E-cadherin, cell adhesion and ultimately of connexin-mediated cell communication in the proximal tubule under diabetic conditions; these changes occur ahead of overt signs of renal damage.

Keywords Cell adhesion · Cell communication · Diabetic nephropathy · Epithelial-to-mesenchymal transition · Fibrosis · Gap junctions · Proximal tubule

C. E. Hills (✉) · P. E. Squires
School of Life Sciences, University of Warwick,
Coventry CV4 7AL, UK
e-mail: C.hills@warwick.ac.uk

E. Siamantouras · K.-K. Liu
School of Engineering, University of Warwick,
Coventry, UK

S. W. Smith · P. Cockwell
Department of Renal Immunobiology,
Institute of Biomedical Research, University of Birmingham,
Birmingham, UK

Abbreviations

EMT	Epithelial-to-mesenchymal transition
GJ	Gap junction
GJIC	Gap junctional intercellular communication
HK	Human kidney cell line
hPTC	Human proximal tubule cells
siRNA	Small interfering RNA
SMAD	Small mothers against decapentaplegic

TBM   Tubular basement membrane
TBR   Transforming growth factor beta receptor

Introduction

The crucial pathology underlying progressive chronic kidney disease in diabetes is tubulointerstitial fibrosis [1, 2]. Central to this process is epithelial-to-mesenchymal transition (EMT) or the trans-differentiation of tubular epithelial cells into myofibroblasts [3–5]. Overwhelming evidence implicates TGF-β1 as the predominant cytokine mediating these phenotypical fibrotic changes [6, 7]. In diabetes, production of TGF-β1 in the proximal tubule is stimulated by high glucose [8, 9]. TGF-β1 modulates the production of several epithelial cell recognition and organisational proteins, while contributing to the reciprocal loss of tubular epithelial cells and accumulation of interstitial fibroblasts, changes associated with declining excretory function [10–12]. In EMT, the loss of epithelial characteristics, e.g. epithelial (E)-cadherin and the zonula occludens protein-1, coincides with the acquisition of proteins associated with a mesenchymal phenotype, e.g. α-smooth muscle actin, fibroblast-specific protein and vimentin, a process that culminates in cytoskeletal remodelling and disruption of the tubular basement membrane [13, 14]. Loss of cell adhesion, associated with reduced E-cadherin levels, represents a pivotal step in those early phenotypical and morphological changes previously observed in response to TGF-β1-induced tubular injury [15]. Cadherins have a central role in forming the multi-protein adherens junction that links cell-to-cell contact to the actin cytoskeleton and various other signalling molecules [16]. The extracellular domain mediates ligation with E-cadherin on adjacent cells [17], while the cytoplasmic domain binds to β-catenin, linking cadherin to the actin cytoskeleton via α-catenin. Interaction, via the catenins, of cadherin with F-actin not only increases the adhesive strength of the junction, but also acts as a signalling 'node' for proteins that influence adhesiveness and/or initiate intracellular signalling. Co-localised with E-cadherin and β-catenin at the sites of cell-to-cell contact [18], connexins oligomerise into hexameric hemichannels (connexons) that connect the cytoplasm of adjoining cells and form gap junctions (GJs). Gap junctions allow transfer of solutes, metabolic precursors and electrical currents [19], and are essential for synchronising activity to ensure appropriate function. Inhibition of cadherin-based cell adhesion inhibits GJ assembly [20], while production of recombinant cadherins into cells lacking strong coupling increases connexin phosphorylation at the adherens junction [21] and increases cell-to-cell communication [22]. Since intercellular adhesion precedes GJ formation and inhibition of cadherin-based cell adhesion is known to inhibit GJ assembly, we hypothesised that glucose-evoked increases in TGF-β would compromise cell communication and function in the proximal tubule.

In retinal capillaries of diabetic mice, connexin-43 production is reduced and apoptosis increased, resulting in a loss of cell communication, and in a decline in the number of pericytes and acellular capillaries [23]. This suggests that a loss of connexin production may be crucial in the development of the vascular lesions observed in diabetic retinopathy. Similar findings from vascular endothelial cells confirm that high glucose decreases connexin production and function, and that this is an early trigger of apoptosis [24]. These data highlight the importance of GJ-mediated cell coupling and suggest that a loss of cell-to-cell communication may contribute to some microvascular complications of the disease. Glucose decreases GJ conductance and disrupts cellular homeostasis in various cell systems [25, 26], and glucose-dependent downregulation of connexin-43 and of GJ communication has been reported in bovine retinal pericytes [27], and in endothelial [28, 29] and epithelial cells [30]. While the presence of GJs in the kidney has long been known, details on their function in the proximal tubule are sparse. Studies on renal vasculature have confirmed a role for various connexins in renin secretion and the regulation of blood pressure [31], but minimal data exist on their role in tubular function, where levels are also high. The novel findings presented here demonstrate a link between high glucose, TGF-β1, impaired cell adhesion and reduced GJ abundance in the proximal tubule. These changes have profound effects on overall cellular integrity and function, and may be among the key events orchestrating loss of function in diabetic nephropathy.

Methods

Materials for tissue culture Tissue culture supplies were purchased from Invitrogen (Paisley, UK). Immobilon P membrane was from Millipore (Watford, UK) and electrochemoluminescence from Amersham Biosciences (Amersham, UK). A Qproteome kit was obtained from Qiagen (Crawley, UK). Antibodies and small interfering RNA (siRNA) were obtained from Santa Cruz (Santa Cruz, CA, USA), R&D Systems (Abingdon, UK) and Affinity Bioreagents (Cambridge, UK). Recombinant human TGF-β1, fibronectin, lipofectamine and Lucifer yellow were obtained from Sigma (Poole, UK), as were all other general chemicals. The anti-TGF-β1 ELISA was from R&D Systems.

Model cell line Human kidney cell line (HK)2 cells (passages 18–30) were maintained in DMEM/Hams F12 medium, which was supplemented with 10% FCS wt/vol, glutamine (2 mmol/l) and EGF (5 ng/ml), and were cultured

at 37°C in a humidified atmosphere with 5% CO_2. Prior to treatment, cells were transferred to DMEM/F12 low glucose (5 mmol/l) for 48 h as described previously [32]. Cells were serum-starved overnight before applying either TGF-β1 (2–10 ng/ml), anti-E-cadherin-neutralising antibody (20 μg/ml) or anti-N-cadherin-neutralising antibody (10 μg/ml) for 48 h. To assess the effect of high glucose, cells were treated with 5 mmol/l (control), 25 mmol/l (high) glucose or 25 mmol/l mannitol (osmotic control) for 48 h or 7 days.

Human proximal tubular cells Following patient consent and ethical approval from South Staffordshire Research Ethics Committee (application number 08/H1203), cells were obtained from anonymised nephrectomy procedures for renal carcinoma. Renal cortex was longitudinally sectioned, the fibrous capsule removed and 1 cm^3 portions cut from the outer region. Pieces were placed into DMEM and further cut into 1 mm^3 sections. Each piece was placed into a well of a 24-well plate that had been previously coated with gelatine for 20 min, followed by incubation in FCS overnight. Sections were cultured in DMEM/Nutrient Ham's F12 1:1, which was supplemented with 5 mg/ml insulin, 5 mg/ml transferrin, 5 ng/ml sodium selenite, 36 ng/ml hydrocortisone, 4 pg/ml triiodothyronine, 10 ng/ml EGF, 2 mmol/l glutamine, 10,000 U/ml penicillin and 10,000 mg/ml streptomycin. Culture was at 37°C in atmosphere with 5% CO_2. Immunohistochemical staining showed cells to be positive for cytokeratin, human epithelial antigen and alkaline phosphatase, but negative for factor VIII-related antigen and actin.

Quantification of TGF-β1 Total TGF-β1 was measured by specific ELISA of cell culture supernatant fractions collected from growth-arrested HK2 cells stimulated under serum-free conditions. Active TGF-β1 was measured directly, while latent TGF-β1 was measured indirectly following acid activation of samples. The assay used has <1% cross-reactivity for TGF-β2 and TGF-β3. The TGF-β1 concentration was normalised to mg/ml of protein. Quantities of TGF-β1 are expressed as pg ml^{-1} (mg protein)$^{-1}$.

Immunoblotting Cytosolic proteins were prepared and separated by gel electrophoresis and electro-blotting on to Immobilon P membranes as described previously [32]. For determination of protein localisation, proteins were collected using the Qproteome (Qiagen) cell compartment kit. Membranes were probed with specific polyclonal antibodies against anti-E-cadherin (R&D Systems), N-cadherin (Sigma), snail (R&D Systems), vimentin (Affinity Bioreagents), β-catenin (Santa Cruz) and connexin-43 (Santa Cruz) at dilutions of 1:1,000, 1:500, 1:500, 1:800, 1:1,000 and 1:400 respectively.

Connexin-43 knockdown Cells were grown to 40% confluence in six-well plates or on cover-slips treated with
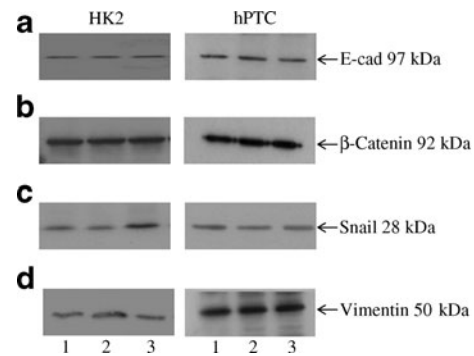

Fig. 1 HK2 and hPTC produce adherens junction proteins. Western blot analyses of HK2 and hPTC cell lysates (5 μg protein/lane) using antibodies against human (**a**) E-cadherin (E-cad), (**b**) β-catenin, (**c**) snail and (**d**) vimentin detected appropriate bands as labelled. Controls included antibody pre-absorbed with a tenfold excess of immunising peptide (data not shown)

3-aminopropyltriethoxy-silane. Knockdown of *CX43* (also known as *GJA1*) expression was achieved using siRNA. Transfection of siRNAs was carried out using lipofectamine as described previously [33]. Cells were collected and assayed at 48, 72 and 96 h after transfection. Negative controls included untransfected cells, lipid alone, and two scrambled siRNAs, one of which was fluorescein-conjugated. *CX43* knockdown was confirmed by Western blot analysis.

Immunocytochemistry Cells at 80% confluence were fixed with 4% paraformaldehyde. After blocking, the nuclear stain DAPI (1 mmol/l) was added for 3 min. Cells were then either incubated for 1 h at 25°C with tetramethyl rhodamine isothiocyanate (TRITC)-conjugated phalloidin (Sigma), diluted at 1:100, in PBS-Triton, or they were incubated overnight at 4°C with primary antibody (1:100) diluted in PBS-Triton. Candidate proteins were visualised using Alexa488-conjugated secondary antibody (1:400) in PBS-Triton for 1 h at 25°C. Fluorescence was visualised using a fluorescence
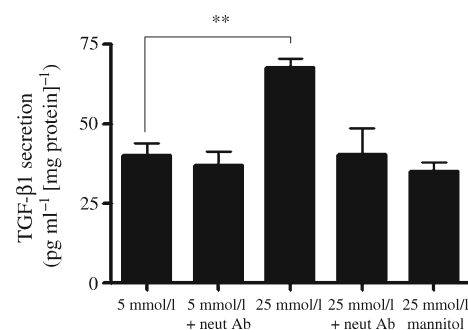

Fig. 2 High glucose stimulates TGF-β1 secretion in HK2 cells. HK2 cells were grown in either low glucose (5 mmol/l, control) or high glucose (25 mmol/l) with or without TGF-β1-neutralising antibody (neut Ab; 10 μg/ml) for 7 days under serum-free conditions. Mannitol (25 mmol/l) was used as an osmotic control. The supernatant fraction was removed and TGF-β1 secretion quantified by ELISA. Results are representative of three separate experiments; **$p<0.01$

microscope (Axiovert 200; Carl Zeiss, Welwyn Garden City, UK).

Dye transfer Lucifer yellow was dissolved in 250 μl fresh LiCl (150 mmol/l) with HEPES (10 mmol/l; pH 7.2). Individual cells within a cell cluster were injected using a delivery system (Injectman/Femtojet 5247; Eppendorf, Hamburg, Germany). The duration of injection was set at 1 s, with an injection pressure of 14,000 Pa and a compensation pressure of 4,800 Pa. Dye transfer between coupled cells was recorded over 4 min using a software package (Metamorph; Molecular Devices, Sunnyvale, California, USA) and a Cool Snap HQ CCD camera (Roper Scientific, Gottingen, Germany).

Single cell force spectroscopy Atomic force microscope force spectroscopy (CellHesion module; JKP Instruments, Berlin, Germany) was used to measure cell-to-cell adhesion and the separation forces required to uncouple these cells. A single HK2 cell was bound to a cantilever using fibronectin (20 mg/ml) and poly-L-lysine (25 μg/ml), and subsequently brought into contact with an adherent cell (in a cluster of coupled cells) using a known force (1 nN). The two cells remained in contact for a defined period of time (10 s) while bonding formed. The cantilever was then retracted at a constant speed (5 μm/s), and force (in nanonewton) versus displacement (deflection of the cantilver) was measured using a laser until the cells were completely separated (pulling length 60–80 μm). Each cell–cell recording was repeated in triplicate with a 30 s interval between successive measurements. Retraction recordings from multiple cells (approx. 50) in separate experiments ($n=5$) were made and the maximum unbinding force (in nanonewton) and detachment energy (in femtojoules) calculated.

Statistical analysis Autoradiographs were quantified by densitometry using a device (TotalLab 2003; NonLinear Dynamics, Durham, NC USA). Where data were quantified,
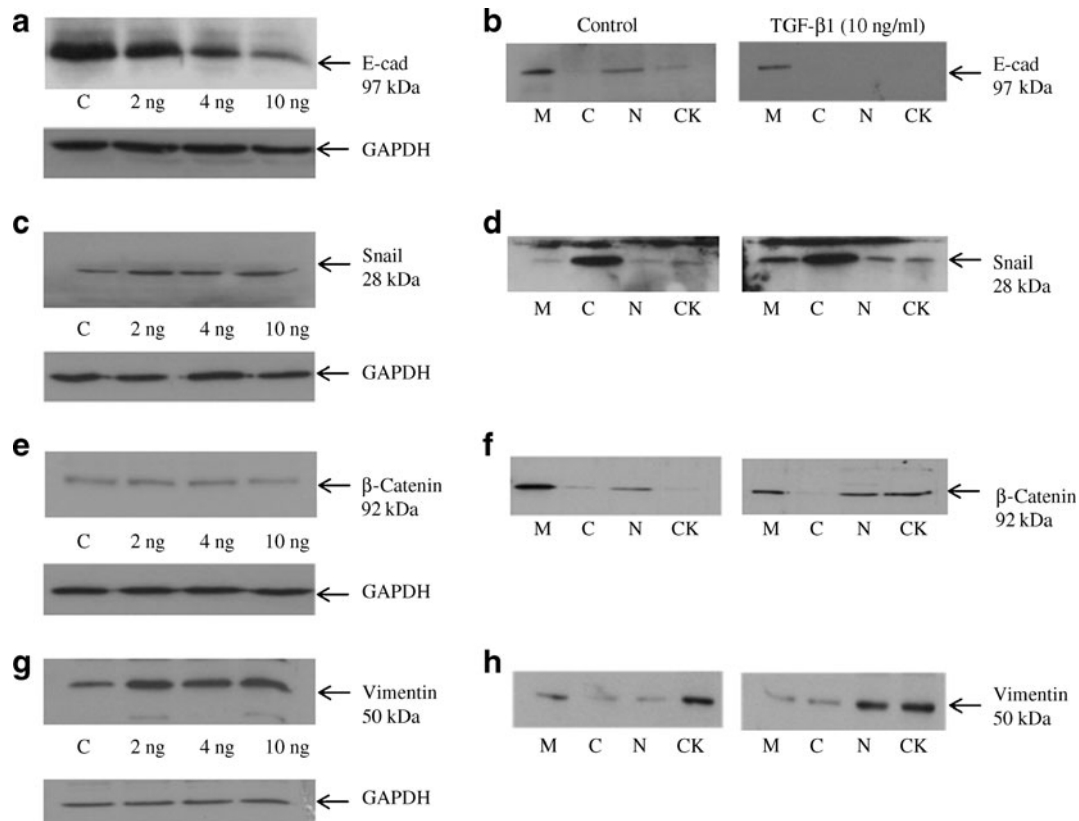

Fig. 3 TGF-β1 evoked changes in adherens junction protein abundance in HK2-cells. **a, c, e, g** To assess the effect of TGF-β1 on production of key adherens junction proteins, HK2 cells were grown in low glucose (5 mmol/l) alone (control [C]), or together with 2, 4 or 10 ng/ml TGF-β1. Whole-cell abundance of E-cadherin (E-cad) (**a**) and its transcriptional co-repressor snail (**c**) was determined by immunoblotting. TGF-β1 decreased E-cadherin levels (**a**) and reciprocally increased the abundance of snail (**c**). **b** Compartmental localisation of E-cadherin and (**d**) snail production was determined in membrane (M), cytosol (C), nuclear (N) and cytoskeletal (CK) fractions of HK2 cells with or without TGF-β1 (10 ng/ml). The cytokine altered the cellular localisation of both proteins compared with control. **e** The cytokine did not alter whole-cell production of β-catenin, but (**g**) did increase vimentin abundance in a concentration-dependent manner. **f** The distribution of β-catenin and (**h**) vimentin between the different cell compartments was altered in response to TGF-β1. Representative blots for each protein were re-probed for GAPDH as a loading control

the non-stimulated, low-glucose control condition was normalised to 100% and data from all other experimental conditions compared with this. Statistical analysis of data was performed using a one-way ANOVA test with Tukey's multiple comparison post-test. Data are expressed as mean± SEM, with 'n' denoting the number of experiments. A value of $p<0.05$ was taken to signify statistical significance.

Results

HK2 and human proximal tubule cells produce adherens junction proteins Western blot analysis confirmed that E-cadherin, β-catenin, snail and vimentin are produced in HK2 and human proximal tubule cells (hPTC), giving rise to bands at 97, 92, 28 and 50 kDa respectively (Fig. 1).

High glucose increases secretion of TGF-β1 ELISA of supernatant fractions from HK2 cells showed a 68% increase in total TGF-β1 secretion (67±2.9 pg/ml [mean±SEM]) after exposure to high glucose (25 mmol/l) for 7 days under serum-free conditions (Fig. 2) compared with exposure to 5 mmol/l glucose (40±3.9 pg/ml; $n=3$; $p<0.01$). Differences in TGF-β1 were only detected following acidification of the samples, suggesting that TGF-β1 was produced in its latent form. Incubation with a TGF-β1-neutralising antibody

(10 μg/ml) blocked the effects of high glucose, restoring TGF-β1 secretion to basal (40±8.2 pg/ml). Mannitol (25 mmol/l) failed to increase TGF-β1 secretion. There was no difference in TGF-β1 secretion in supernatant fractions taken from cells exposed to high glucose for 48 h (data not shown).

TGF-β1 alters adherens junction protein abundance in HK2-cells TGF-β1 (2–10 ng/ml for 48 h) altered cell morphology from an epithelial-like cobblestone appearance, to an elongated fibroblast-like phenotype (electronic supplementary material [ESM] Fig. 1a). These changes were accompanied by re-organisation of the actin cytoskeleton into peripheral stress fibres (ESM Fig. 1b). The cytokine (2–10 ng/ml for 48 h) induced a concentration-dependent decrease in whole-cell abundance of E-cadherin (Fig. 3a), attributable to reduced production from the membrane and nuclear cell compartments (Fig. 3b). In contrast, TGF-β1 increased levels of the transcriptional repressor snail throughout the cell (Fig. 3c, d). Integral to E-cadherin cell adhesion under basal conditions, β-catenin was primarily localised at the membrane (Fig. 3f). In the current study, TGF-β1 failed to alter whole-cell production of β-catenin (Fig. 3e), but did redistribute the catenin from the membrane to the nuclear and cytoskeletal fractions (Fig. 3f). TGF-β1 produced a concentration-dependent increase in whole-cell levels of the intermediate filament protein, vimentin (Fig. 3g), with the greatest change in the cytoskeleton and nucleus (Fig. 3h).

Fig. 4 TGF-β1 evoked changes in adherens junction protein abundance in hPTCs. hPTCs were grown in low glucose (5 mmol/l) with or without TGF-β1 (2–10 ng/ml) for 48 h and whole-cell abundance of (**a**) E-cadherin (E-cad), (**b**) snail, (**c**) vimentin and (**d**) β-catenin was determined by immunoblotting. Representative blots are shown for each protein with re-probing for GAPDH done as loading control. Quantification (mean± SEM) was by densitometry, normalised against the non-stimulated low glucose control (100%). Bars in the histograms correspond to the associated lanes in the respective blot. Results were from three or more separate experiments; *$p<0.05$, **$p<0.01$ and ***$p<0.001$
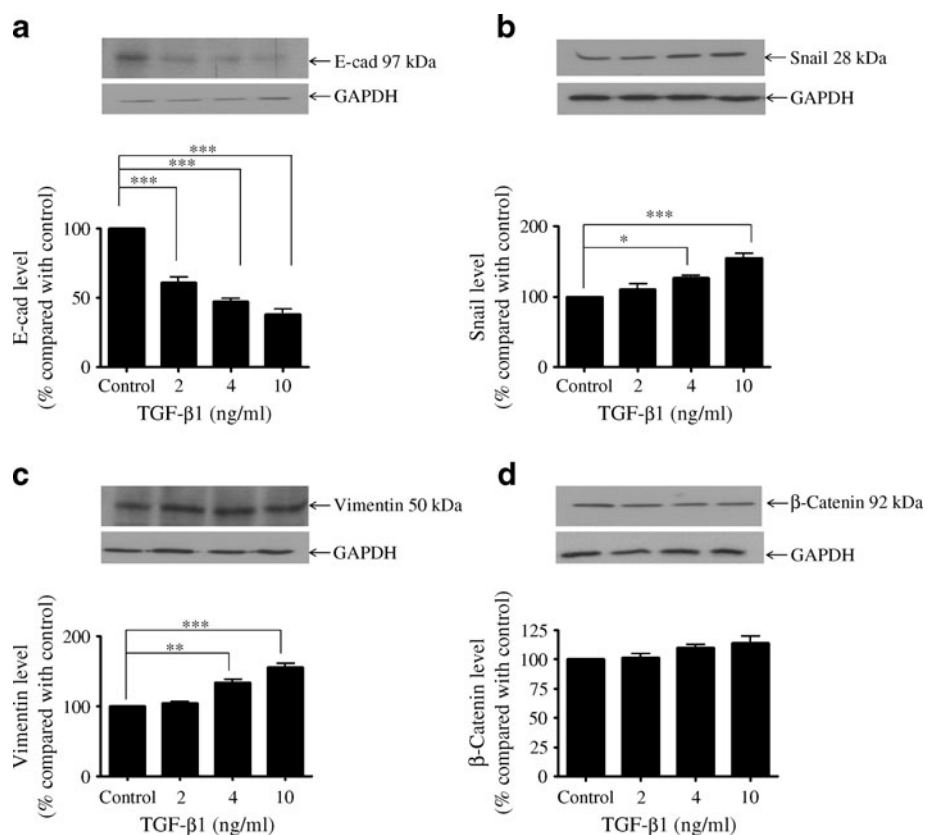
TGF-β1 alters adherens junction protein abundance in hPTC Human proximal tubule cells were incubated for 48 h in low glucose (5 mmol/l) with increasing concentrations of TGF-β1 (2–10 ng/ml). TGF-β1 reduced levels of E-cadherin by 68±3.7% (mean±SEM), 51±2.3% and 45±4.6% of control at 2, 4 and 10 ng/ml respectively ($n=3$; $p<0.001$) (Fig. 4a). It also upregulated snail production to 110±10.4%, 127±7.8% ($n=3$; $p<0.05$) and 154±8.5% ($n=3$; $p<0.01$) of control (Fig. 4b), but failed to alter the production of β-catenin (Fig. 4d). Production of the intermediate filament protein, vimentin, increased to 104±7.5%, 133±9.4% and 155±8.4% of control at 2, 4 and 10 ng/ml ($n=3$; $p<0.01$) (Fig. 4c).

TGF-β1 decreases connexin-43 production Following in vitro activation of latent TGF-β1 by repeated freeze–thaw cycles in 7 day conditioned medium [34], a subsequent 48 h exposure of cells to the activated medium significantly decreased connexin-43 levels to 72±2.1% (mean±SEM) of that with conditioned 5 mmol/l control medium ($n=3$; $p<0.05$) (Fig. 5a). Mannitol (25 mmol/l) failed to alter connexin-43 production. In Fig. 5b, TGF-β1 (48 h) decreased connexin-43 abundance in HK2 cells to 40±6.1%, 37±7.9% and 30±12.6% of control at 2, 4 and 10 ng/ml ($n=3$; $p<0.001$). These data were comparable to the cytokine-induced inhibition of connexin-43 in hPTC, where levels fell to 53±4.8%, 53±3.7% and 51±3.5% of control at similar concentrations of TGF-β1 ($n=3$; $p<0.001$) (Fig. 5c). In the absence (Fig. 5d) or presence (Fig. 5e) of the cytokine (10 ng/ml), connexin-43 was predominantly localised to the cell membrane. The reduction of whole-cell abundance of the protein therefore reflects a decrease in production, rather than redistribution to other cell compartments.
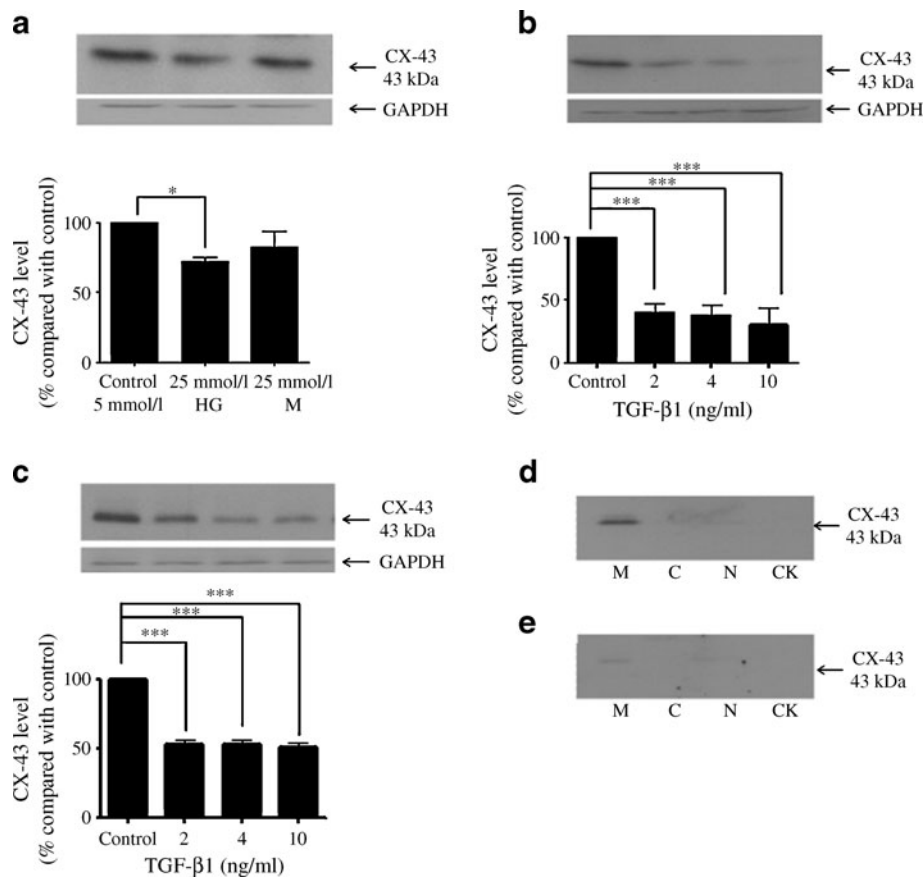

Fig. 5 TGF-β1 downregulates connexin-43 levels in proximal tubule cells. To assess the effects of glucose on connexin-43 (CX-43) abundance, HK2 cells were cultured (**a**) in either low glucose (5 mmol/l, control), high glucose (HG, 25 mmol/l) or mannitol (M, 25 mmol/l) for 7 days. Secreted TGF-β1 was activated by repeat freeze–thaw procedure and the conditioned medium applied for 48 h. **b** In a separate series of experiments, HK2 and (**c**) hPTC cells were grown in low glucose (5 mmol/l) with or without 2, 4 or 10 ng/ml TGF-β1. Whole-cell connexin-43 abundance was determined by immunoblotting. The representative immunoblots show changes in protein production versus the same blots stripped and re-probed for GAPDH as a loading control. Blots were quantified (mean±SEM) by densitometry data from three or more separate experiments and data normalised against the unstimulated low glucose control (100%). Bars in the histograms correspond to the associated lanes in the respective blot. *$p<0.05$ and ***$p<0.001$. **d** Compartmental localisation of connexin-43 production was determined in membrane (M), cytosol (C), nuclear (N) and cytoskeletal (CK) fractions of control and (**e**) TGF-β1-treated (10 ng/ml) HK2 cells

Loss of connexin-43 decreases gap junctional intercellular communication in proximal tubule cells HK2 cells and hPTC produce connexin-43 (Fig. 6a). siRNA was used to knockdown *CX43* expression to 30±3.4% (mean±SEM) of control (*n*=4, *p*<0.001), while scrambled siRNA and transfection reagent alone had no effect (Fig. 6b). In separate experiments, cells were transfected with fluorescein-tagged *CX43* siRNA to identify transfected cells expressing reduced *CX43* (Fig. 6). Injection of Lucifer yellow into the transfected cells failed to exhibit dye transfer (Fig. 6g–j), while dye moved away from the site of injection in nontransfected cells within the same cell cluster, confirming connexin-43-mediated intercellular communication (Fig. 6m–p).
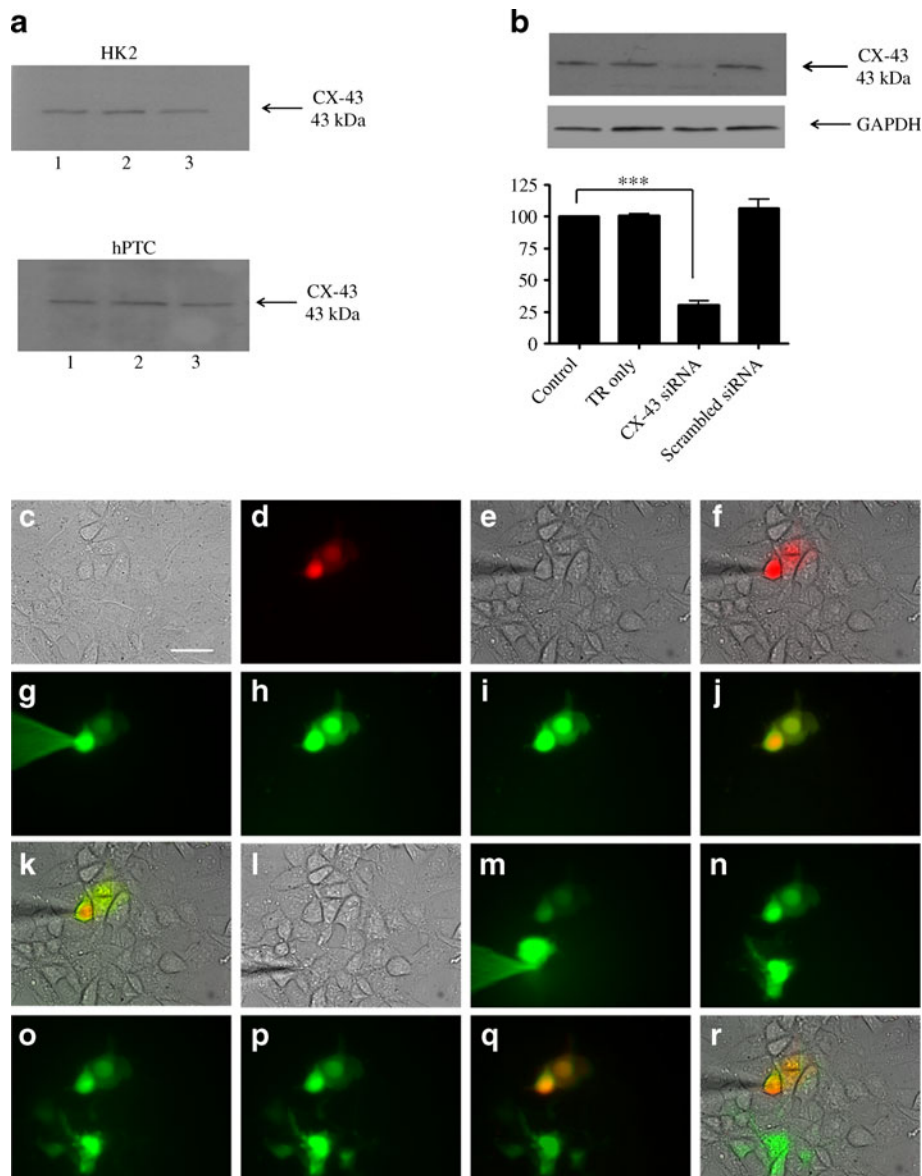

Fig. 6 Knockdown of *CX43* prevents GJIC in HK2 cells. **a** Confirmation of connexin-43 (CX-43) production in three separate preparations from HK2 cells and hPTC. **b** *CX43* siRNA significantly reduced connexin expression in HK2 cells. The representative immunoblot shows changes in protein abundance for the transfection reagent (TR) alone, for *CX43* siRNA and scrambled siRNA versus the same blot stripped and re-probed for GAPDH as a loading control. Blots were quantified by densitometry and data normalised against the non-stimulated low glucose (5 mmol/l; 100%). Bars in the histogram correspond to the associated lanes in the respective blot. Values are mean±SEM from three separate experiments; ***p<0.001. **c** Red fluorescent protein was used to identify cells exhibiting anti-connexin-43 transfection within a cluster of non-transfected cells. The red transfected cell (**d**) was injected (**e**, **f**) with Lucifer yellow (**g**) and dye spread (green) examined between 0 min (**h**) and 4 min (**i**). **j** An overlay (yellow) of red transfection and green dye spread, with phase (**k**) at 4 min after the initial injection of dye. The micro-injector (**l**) was repositioned over a non-transfected cell in the same cluster. **m**, **n** Injection of Lucifer yellow led to spreading of dye (green) between 0 min (**o**) and 4 min (**p**). An overlay (yellow) of red transfection and green dye spread (**q**), with (**r**) a triple overlay with a phase image. Scale bar (**c**) 50 μm

Loss of E-cadherin ligation replicates TGF-β1-induced changes in connexin-43 production To determine whether the reduction in gap junctional intercellular communication (GJIC) induced by TGF-β1 depended on a decrease in E-cadherin production or reflected reduced E-cadherin-mediated ligation between adjacent cells, HK2 cells were treated for 48 h with an immunoneutralising antibody for E-cadherin. The antibody (antiuvomorulin, 20 μg/ml; Sigma) prevents ligation, but has no effect on production of the protein. Neutralisation of E-cadherin ligation altered cell morphology in a manner consistent with those changes observed in response to TGF-β1 (Fig. 7a). The cytokine and anti-E-cadherin significantly downregulated whole-cell abundance of connexin-43 to 43±4.0% (mean±SEM) and 37±7.6% of control ($n=3$; $p<0.001$) (Fig. 7b), an effect mainly attributable to a decrease in production at the membrane (Fig. 7c, d). Co-application of TGF-β1 and anti-E-

cadherin did not potentiate the changes in connexin-43 production compared with TGF-β1 alone (data not shown). Although, as expected, TGF-β1 significantly reduced E-cadherin levels to 32±6.1% of control ($n=3$; $p<0.01$), neutralisation of ligation failed to alter abundance (112.7±12.2% of control; $n=3$) (Fig. 7e) or localisation of E-cadherin (Fig. 7f, g). In agreement with data presented in Figs 3 and 4, TGF-β1 increased the abundance of snail to 125±13.8% of control ($n=3$; $p<0.05$), while neutralisation of E-cadherin ligation had little effect on whole-cell abundance (Fig. 7h) or localisation of the protein (Fig. 7i, j). Whole-cell levels of β-catenin were unchanged by TGF-β1 or loss of E-cadherin ligation; however, the latter re-localised to the cytoskeleton (Fig. 7k–m).

TGF-β1 reduces GJIC in proximal tubule cells HK2 cells were cultured for 48 h in low (5 mmol/l) or high (25 mmol/l)
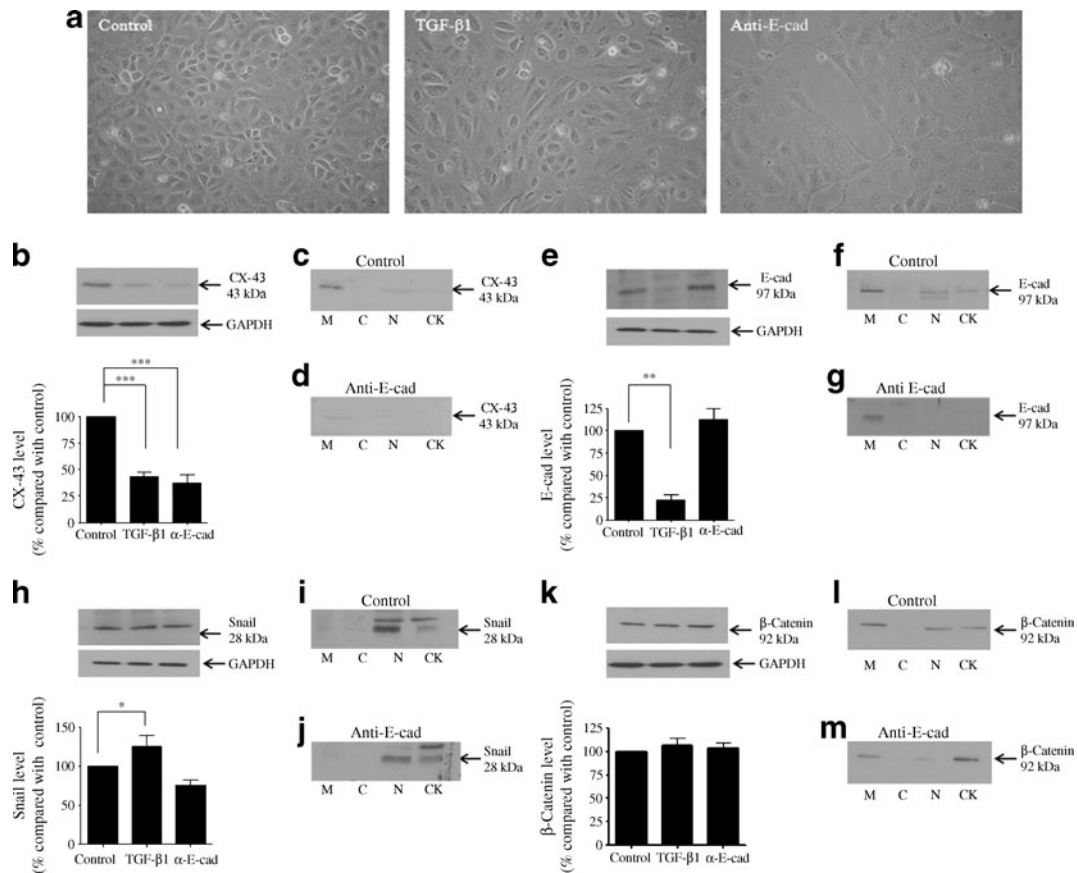

Fig. 7 Loss of E-cadherin (E-cad) ligation partially mimics the effects of TGF-β1 on cell morphology and connexin-43 (CX-43) production in HK2 cells. **a** Phase contrast microscopy demonstrated that TGF-β1 (10 ng/ml) and loss of E-cadherin ligation altered gross cell morphology in favour of a fibroblast phenotype. Magnification ×20. **b–d** The effects of the cytokine and anti-E-cadherin (E-cad) on the abundance of connexin-43, (**e–g**) E-cadherin, (**h–j**) snail and (**k–m**) β-catenin were examined in HK2 whole-cell lysates and cell fractions. Representative immunoblots (**b, e, h, k**) show changes in candidate protein production versus the same blots stripped and re-probed for GAPDH as a loading

control. Blots were quantified by densitometry and data normalised against the unstimulated low glucose (5 mmol/l) control (100%). Bars in the histograms correspond to the associated lanes in the respective blots. Densitometry values are mean±SEM from three or more separate experiments; *$p<0.05$, **$p<0.01$ and *** $p<0.001$. **c, d, f, g, i, j, l, m** Compartmental localisation for each protein as labelled was determined in membrane (M), cytosol (C), nuclear (N) and cytoskeletal (CK) fractions of HK2 cells with or without anti-E-cadherin antibody (20 μg/ml) for 48 h

glucose, and in low glucose with or without TGF-β1 (2–10 ng/ml), or with or without anti-E-cadherin antibody (20 μg/ml). Individual cells within a cluster were injected with Lucifer yellow (green) and the degree of dye spread assessed 4 min after injection (Fig. 8). In control cells, dye permeated away from the injected cell into neighbouring cells (Fig. 8a). This cell–cell coupling was reduced under high (25 mmol/l) glucose conditions (Fig. 8b). TGF-β1 (2–10 ng/ml) produced a concentration-dependent reduction in the extent of dye-transfer (Fig. 8c–e). This loss of GJIC was mimicked in cells treated with anti-E-cadherin (Fig. 8f).
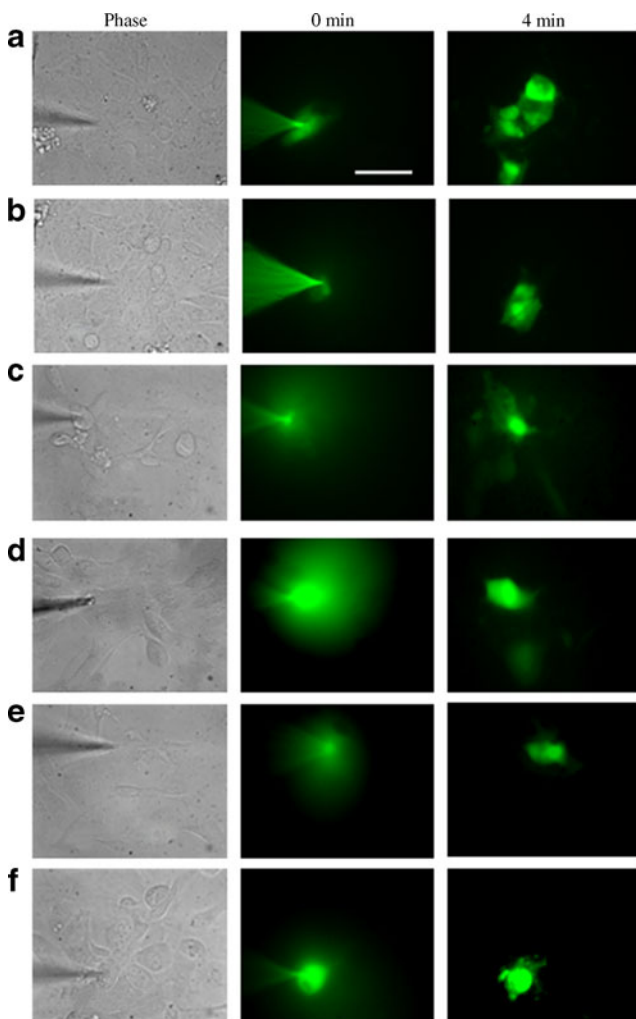

Fig. 8 TGF-β1 reduces GJIC in HK2 cells. GJIC was determined by the extent of dye (green) spread following micro-injection of Lucifer yellow into a single HK2 cell within a cell cluster. **a** Control cells exhibited a rapid (0 to 4 min) transfer of dye between neighbouring cells. **b** Exposure for 48 h to high glucose (25 mmol/) or (**c**) low glucose (5 mmol/l) plus incubation with 2 ng/ml, (**d**) 4 ng/ml and (**e**) 10 ng/ml TGF-β1 evoked a concentration-dependent decrease in dye spread. **f** Neutralisation of E-cadherin ligation using an immunoneutralising antibody (20 μg/ml) also restricted intercellular communication and prevented dye transfer. Scale bar 50 μm

Decreased E-cadherin increases N-cadherin production N-cadherin abundance (135 kDa) (Fig. 9a) was predominantly localised to the cell membrane (Fig. 9b) and was significantly upregulated by TGF-β1 (48 h) to 176±23% (mean± SEM), 280±17% and 325±62% of control at 2, 4 and 10 ng/ml TGF-β1 in HK2 cells ($n=3$; $p<0.05$) (Fig. 9c), and to 237±45%, 240±18% and 305±27.5% of control in hPTC ($n=3$; $p<0.01$) (Fig. 9d). In a separate series of experiments in HK2-cells, TGF-β1 (10 ng/ml) upregulated N-cadherin to 310±66% of control ($n=3$; $p<0.05$) (Fig. 9e), while neutralisation of E-cadherin ligation only increased production to 172±47% of control. The neutralising antibody had little effect on connexin-43 production (91±8.4% of control, $n=3$) (Fig. 9f) compared with TGF-β1 or anti-E-cadherin, which significantly decreased connexin-43 abundance by 54±4.8% and 40±8.9% respectively ($n=3$; $p<0.001$).

TGF-β1 reduces adherence between coupled cells of the proximal tubule Atomic force microscope force spectroscopy was used to measure cell-to-cell adhesion and the separation forces required to uncouple cells. Prior to attachment, cells were cultured for 48 h under identical conditions with or without TGF-β1 (10 ng/ml). A single HK2 cell (cell-1) was bound to a cantilever and subsequently brought into contact with an adherent cell (cell-2) within a cluster, using a fixed force (Fig. 10). After 10 s, the cantilever was then retracted (5 μm/s) and force versus displacement measured until the cells were completely separated. Retraction force–displacement curves provide important information on adhesion between two cells, such as the energy required to separate them (Fig. 10a–c, grey area) and the maximum force of detachment (Fig. 10a–c, red circle). The former is normally referred to as 'detachment energy' (Fig. 10e) and the latter as the 'maximum unbinding force' (Fig. 10d). The retraction measurements of control (47 cells in five separate experiments) and TGF-β1-treated HK-2 cells (53 cells in five separate experiments) are shown in Fig. 10a, b. The results indicate that TGF-β1 decreases the maximum unbinding force by 20±6% (mean±SEM) ($n=5$; $p<0.001$), while the detachment energy was decreased to 53±6% ($n=5$; $p<0.001$). Neutralisation of E-cadherin ligation had minimal effect on detachment energy (112% of control; 47 cells in five separate experiments), but actually increased the maximum unbinding force by 32±0.5% (Fig. 10c).

Discussion

TGF-β1 is important in many tubulointerstitial diseases where disassembly of the adherens junction represents the initial overt change in epithelial organisation, well before
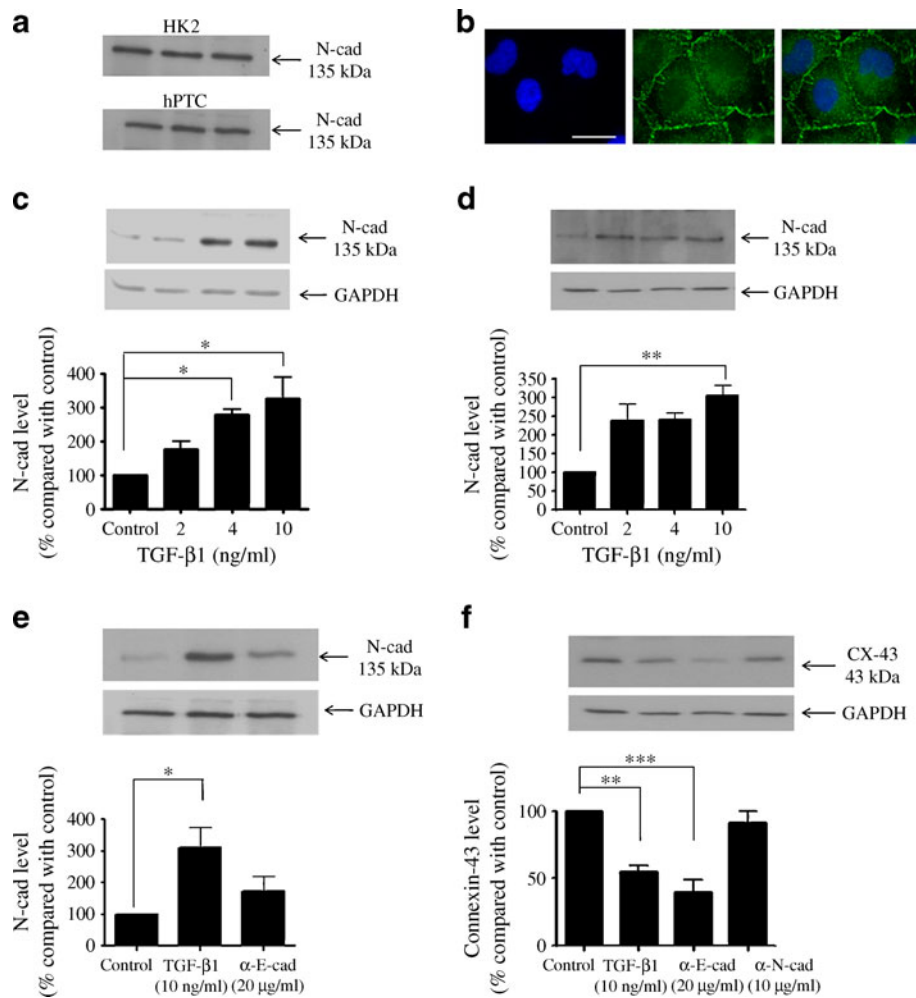
Fig. 9 TGF-β1 turns on the 'cadherin switch'. **a** Western blot analyses of HK2 and hPTC cell lysates (5 μg protein/lane) using antibodies against human N-cadherin (N-cad) detected bands of approximately 135 kDa in three different protein preparations. **b** Membrane localisation was confirmed by immunocytochemistry, where N-cadherin immunoreactivity was visualised by ALEXA488 (green), with nuclear staining by DAPI (blue). Scale bar 10 μm. **c** HK2 cells and (**d**) hPTC were grown in low glucose (5 mmol/l) alone or with 2, 4 or 10 ng/ml TGFβ-1 for 48 h, after which whole-cell abundance of N-cadherin was determined by immunoblotting. **e** Comparison of the effects of TGF-β1 and anti-E-cadherin (E-cad) on N-cadherin levels, and (**f**) of the effects of TGF-β1, anti-E-cad and anti-N-cadherin on connexin-43 levels in HK2 cells. The representative immunoblots show changes in protein abundance. The same blots were stripped and re-probed for GAPDH as a loading control. Blots were quantified by densitometry and normalised against the non-stimulated low glucose control (100%). Bars in histograms correspond to the associated lanes in the respective blots. Densitometry data are mean±SEM from three or more separate experiments; *$p<0.05$, *$p<0.01$ and ***$p<0.001$

any suggested cellular migration associated with EMT [34, 35]. The cadherin–catenin complex is crucial in epithelial cell-to-cell adhesion and facilitates cell communication via GJs. We confirm that TGF-β1 reduces membrane abundance of E-cadherin, and show for the first time that the cytokine decreases functional tethering between cells of the proximal tubule. While TGF-β1 fails to alter whole-cell production of β-catenin, accumulation in the nucleus is synonymous to that shown previously, and may signify release and subsequent re-localisation of β-catenin in response to reduced levels of cadherin [36]. Our data provide compelling evidence that cell-to-cell adhesion and connexin-43 GJIC are dramatically reduced in the presence

of TGF-β1, events likely to represent an early stage in glucose-induced renal damage in the proximal tubule.

To establish a direct link between E-cadherin and connexin-43 production, a neutralising antibody against E-cadherin ligation was used to mimic changes in cell adhesion seen in response to TGF-β1. Negation of E-cadherin ligation did not affect production of the protein, nor did it upregulate the transcriptional repressor snail, a process that accompanied the downregulation of E-cadherin production in response to TGF-β1. Importantly, however, loss of ligation reduced connexin-43 levels to a comparable degree to that observed in response to the cytokine, suggesting that it is a loss of tethering between cells, rather than a change in
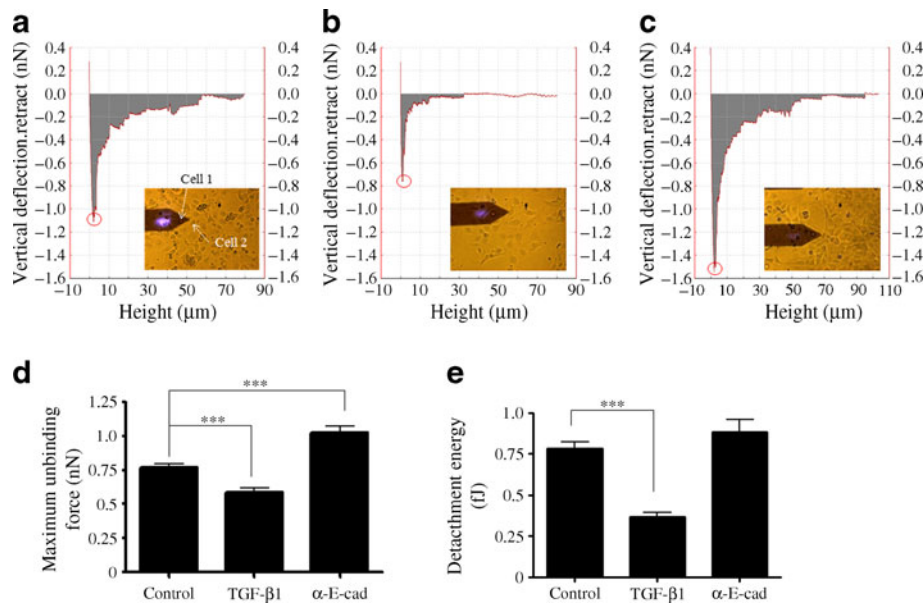
Fig. 10 TGF-β1 reduces cell adhesion. Atomic force microscopy force spectroscopy was used to measure the detachment energy (in femtojoules) and maximum unbinding force (in nanonewton) required to uncouple two HK2 cells. **a** A single HK2 control cell was bound to the cantilever (Cell 1, phase insert). This was brought into contact with an adherent cell (Cell 2) using a fixed force (1 nN) for 10 s, while bonding formed. The cantilever was then retracted (5 μm/s) and force versus displacement measured until the cells separated (approximate pulling length 60 to 80 μm). The energy required to separate the cells (grey area) and the maximum force of detachment (red circle) was measured. Values for height (in micrometres) were smoothed. **b** The same procedure was repeated after treatment with TGF-β1 and (**c**) anti-E-cadherin (E-cad). **d** Quantification of maximum unbinding force' and (**e**) 'detachment energy', showing that TGF-β1 (10 ng/ml) decreased the maximum unbinding force by 20% and the detachment energy decreased by 53% compared with control. Data are expressed as mean±SEM of multiple cells from five separate experiments; ***$p<0.001$

protein abundance as such that controls connexin production and GJIC. Retraction force–displacement curves confirmed that TGF-β1 reduced the maximum unbinding force required to begin separation of two cells by 20%, while halving the detachment energy required to completely separate them. The greater decrease in the detachment energy could be partly explained by the increase in cell rigidity following TGF-β1 treatment, as demonstrated by the rearrangement of the cytoskeleton into peripheral stress fibres (ESM Fig. 1).

A switch in cadherin isoform from E-cadherin to neural (N)-cadherin is associated with EMT [37]. TGF-β1 dramatically increased N-cadherin production in our model. However, this switch was unable to reverse morphological changes or the reduction in cell-to-cell adhesion in response to the cytokine. Surprisingly, neutralisation of E-cadherin ligation actually increased the maximum unbinding force. Counter-intuitively, this observation suggests that the modest increase in N-cadherin evoked by blocking E-cadherin ligation (Fig. 9e) can maintain tethering between coupled cells when the cadherin–catenin complex is intact, i.e. when only ligation is impaired. However, TGF-β1 dramatically reduced E-cadherin production and forced β-catenin to move away from the membrane. In this scenario, and in the absence of a catenin binding partner, upregulation of

N-cadherin is redundant and the switch is unable to maintain tethering. These data suggest that it is decreased E-cadherin production and dissolution of the catenin–cadherin complex that drive the detachment of cells in EMT.

Type 2 EMT is commonly defined as the ability of adult epithelial cells to undergo de-differentiation, traverse the tubular basement membrane (TBM) into the interstitium and trans-differentiate into a myofibroblast phenotype that is capable of synthesising and increasing the deposition of extracellular matrix. While these activated myofibroblasts are thought of as key effector cells in the pathogenesis of renal fibrosis, it is clear that they originate from multiple lineages. Accumulating evidence suggests that local interstitial fibroblasts [38], pericytes [39], local mesenchymal stem cells [40] or the injured epithelium itself [10] may contribute to this pool, and there is considerable debate for and against a role of EMT in renal fibrosis [41]. The established criteria supporting a role of EMT in fibrosis are based on the identification of morphological changes and altered levels of key epithelial/mesenchymal markers. Failure of fibroblasts to fully migrate and traverse the TBM is more commonly known as partial EMT, a phenomenon where cells produce epithelial and mesenchymal markers, yet lack migratory capacity. The argument against full phenotypic transformation has been fuelled by data from Humphreys et al., who suggest that not only is EMT unlikely to

occur in vivo, but that vascular pericytes are the source of fibrosis-generating myofibroblasts [39].

As summarised in a recent review, TGF-β1 binds to a trans-membrane TGF-β receptor II (TBRII) and initiates several intracellular signalling cascades, including small mothers against decapentaplegic (SMAD) and mitogen-activated protein kinases such as extracellular regulated kinase, p38 and Jun kinase [42]. SMADs are subdivided into three classes: (1) receptor regulated SMADs (SMAD1, -2, -3, -5 and −8); (2) the common SMADs (SMAD4); and (3) the inhibitory SMADs (SMAD6 and −7) [43]. Following TBRII activation, receptor-regulated SMADs form oligomeric complexes with the common SMAD prior to translocation into the nucleus and regulation of gene transcription. The majority of TGF-β1-targeted genes that are regulated in EMT rely on SMAD3-dependent transcriptional regulation. Recent studies in cells from the proximal tubule have demonstrated that angiotensin II-induced tubular EMT was SMAD3-dependent [44]. Similarly, (β)1-integrin gene expression, a potential therapeutic target for renal fibrosis, is also upregulated in unilateral obstruction and in chronic tubulointerstitial fibrosis via a SMAD3-dependent mechanism [45]. However, despite the predominant involvement of SMAD3, a role for SMAD2 should not be discounted [46].

The hyperactive SMAD-signalling observed in certain types of renal disease reflects aberrant levels of both SMAD co-repressors and their subsequent regulators [47]. The inhibitory SMADs (SMAD6 and SMAD7) inhibit receptor-regulated SMAD phosphorylation by blocking their access to TBRI, and/or by promoting degradation of the receptor complexes. SMAD7 represents a general antagonist of TGF-β1 and bone morphogenic protein signalling, with reports showing that induction of SMAD7 blocks tubular EMT and the development of fibrotic lesions [48]. The role and regulation of SMAD signalling in regulation of GJ expression and GJIC in the proximal tubule remain to be confirmed; however, it is highly likely that these effects are SMAD-dependent and subject to regulation via endogenous inhibitors. The potential of exogenous agonist application to reverse these disrupted changes in cell-to-cell communication represents an area of therapeutic interest and forms the basis of our continuing research.

Reduced cell adhesion, cell coupling and cell-to-cell communication have profound effects on overall integrity and function of the proximal tubule, and altered GJIC and renal haemodynamics have recently been reported in a Zucker fatty rat model of type2 diabetes [49]. In the current study, we concede that our in vitro data provide a minimalistic model of the early events in EMT and thus recommend caution in translating these novel findings to the in vivo situation, where the multifactorial molecular pathology of renal fibrosis may modify responses. However, despite this caveat, our current data provide a compelling foundation for the identification of future therapies aimed at maintaining or restoring renal function in diabetes, a supposition supported by recent data from mesangial cells, where glucose-induced hypertrophy was reversed by overproduction of connexin-43 [50].

Duality of interest The authors declare that there is no duality of interest associated with this manuscript.

Contribution statement All authors contributed to the conception, design and analysis of the data, and to the drafting of the manuscript, and have approved the final version for publication.

References

1. Eddy AA (1996) Molecular insights into renal interstitial fibrosis. J Am Soc Nephrol 12:2495–2508
2. Remuzzi G, Ruggenenti P, Benigni A (1997) Understanding the nature of renal disease progression. Kidney Int 51:2–15
3. Iwano M, Plieth D, Danoff TM, Xue C, Okada H, Neilson EG (2002) Evidence that fibroblasts derive from epithelium during tissue fibrosis. J Clin Invest 110:341–350
4. Okada H, Danoff TM, Kalluri R, Neilson EG (1997) Early role of Fsp1 in epithelial–mesenchymal transformation. Am J Physiol 273:F563–F574
5. Hills CE, Squires PE (2010) TGF-beta1-induced epithelial-to-mesenchymal transition and therapeutic intervention in diabetic nephropathy. Am J Nephrol 31:68–74
6. Kanwar YS, Wada J, Sun L et al (2008) Diabetic nephropathy: mechanisms of renal disease progression. Exp Biol Med 233:4–11
7. Sharma K, Ziyadeh FN (1995) Hyperglycaemia and diabetic kidney disease. The case for transforming growth factor-beta as a key mediator. Diabetes 44:1139–1146
8. Oldfield MD, Bach LA, Forbes JM et al (2001) Advanced glycation end products cause epithelial-myofibroblast transdifferentiation via the receptor for advanced glycation end products (RAGE). J Clin Invest 108:1853–1863
9. Qi W, Chen X, Zhang Y et al (2007) High glucose induces macrophage inflammatory protein-3 alpha in renal proximal tubule cells via a transforming growth factor-beta 1 dependent mechanism. Nephrol Dial Transplant 11:3147–3153
10. Mauer SM, Steffes MW, Ellis EN, Sutherland DE, Brown DM, Goetz FC (1984) Structural functional relationships in DN. J Clin Invest 74:1143–1155
11. Steffes MW, Osterby R, Chavers B, Mauer SM (1989) Mesangial expansion as a central mechanism for loss of kidney function in diabetic patients. Diabetes 38:1077–1081
12. Hills CE, Al-Rasheed N, Al-Rasheed N, Willars GB, Brunskill NJ (2009) C-peptide reverses TGF-beta-1 induced changes in renal proximal tubular cells: implications for treatment of DN. Am J Physiol 296:F614–F621

13. Bakin AV, Tomlinson AK, Bhowmick NA, Moses HL, Arteaga CL (2000) Phosphatidylinositol 3-kinase function is required for transforming growth factor beta-mediated epithelial to mesenchymal transition and cell migration. J Biol Chem 275:36803–36810

14. Masszi A, Fan L, Rosivall L et al (2004) Integrity of cell–cell contacts is a critical regulator of TGF-beta 1-induced epithelial-to-myofibroblast transition: role for beta-catenin. Am J Pathol 165:1955–1967

15. Zheng G, Lyons JG, Tan TK et al (2009) Disruption of E-cadherin by matrix metalloproteinase directly mediates epithelial–mesenchymal transition downstream of transforming growth factor-beta1 in renal tubular epithelial cells. Am J Pathol 175:580–591

16. Moreno AP, Berthoud VM, Pérez-Palacios G, Pérez-Armendariz EM (2005) Biophysical evidence that connexin-36 forms functional gap junction channels between pancreatic mouse beta-cells. Am J Physiol Endocrinol Metab 288:E948–E956

17. Boggon TJ, Murray J, Chappuis-Flament S, Wong E, Gumbiner BM, Shapiro L (2002) C-cadherin ectodomain structure and implications for cell adhesion mechanisms. Science 17:1308–1313

18. Fujimoto K, Nagafuchi A, Tsukita S, Kuraoka A, Ohokuma A, Shibata Y (1997) Dynamics of connexins, E-cadherin and alpha-catenin on cell membranes during gap junction formation. J Cell Sci 110:311–322

19. Caton D, Calabrese A, Mas C, Serre-Beinier V, Wonkam A, Meda P (2002) Beta-cell crosstalk: a further dimension in the stimulus-secretion coupling of glucose-induced insulin release. Diabetes Metab 28:3S45–S53

20. Kanno Y, Sasaki Y, Shiba Y, Yoshida-Noro C, Takeichi M (1984) Monoclonal antibody ECCD-1 inhibits intercellular communication in teratocarcinoma PCC3 cells. Exp Cell Res 152:270–274

21. Musil LS, Cunningham BA, Edelman GM, Goodenough DA (1990) Differential phosphorylation of the gap junction protein connexin43 in junctional communication-competent and -deficient cell lines. J Cell Biol 111:2077–2088

22. Mege RM, Matsuzaki F, Gallin WJ, Goldberg JI, Cunningham BA, Edelman GM (1988) Construction of epithelioid sheets by transfection of mouse sarcoma cells with cDNAs for chicken cell adhesion molecules. Proc Natl Acad Sci U S A 85:7274–7278

23. Bobbie MW, Roy S, Trudeau K, Munger SJ, Simon AM, Roy S (2001) Reduced connexin 43 expression and its effect on the development of vascular lesions in retinas of diabetic mice. Invest Opthalmol Vis Sci 51:3758–3763

24. Li AF, Roy S (2009) High glucose induced downregulation of connexin 43 expression promotes apoptosis in microvascular endothelial cells. Invest Opthalmol Vis Sci 50:1400–1407

25. Zhang J, Hill CE (2005) Differential connexin expression in preglomerular and postglomerular vasculature: accentuation during diabetes. Kidney Int 68:1171–1185

26. Zhang JH, Kawashima S, Yokoyama M, Huang P, Hill CE (2006) Increased eNOS accounts for changes in connexin expression in renal arterioles during diabetes. Anat Rec A Discov Mol Cell Evol Biol 288:1000–1008

27. Li AF, Sato T, Haimovici R, Okamoto T, Roy S (2003) High glucose alters connexin 43 expression and gap junction intercellular communication activity in retinal pericytes. Invest Ophthalmol Vis Sci 44:5376–5382

28. Sato T, Haimovici R, Kao R, Li AF, Roy S (2002) Downregulation of connexin 43 expression by high glucose reduces gap junction activity in microvascular endothelial cells. Diabetes 51:1565–1571

29. Fernandes R, Girão H, Pereira P (2004) High glucose downregulates intercellular communication in retinal endothelial cells by enhancing degradation of connexin 43 by a proteasome-dependent mechanism. J Biol Chem 279:27219–27224

30. Gomes P, Malfait M, Himpens B, Vereecke J (2003) Intercellular Ca (2+)-transient propagation in normal and high glucose solutions in rat retinal epithelial (RPE-J) cells during mechanical stimulation. Cell Calcium 34:185–192

31. Hanner F, Sorensen CM, Holstein-Rathlou NH, Peti-Peterdi J (2010) Connexins and the kidney. Am J Physiol Regul Integr Comp Physiol 298:R1143–R1155

32. Hills CE, Bland R, Bennett J, Ronco PM, Squires PE (2006) High glucose up-regulates ENaC and SGK1 expression in HCD-cells. Cell Physiol Biochem 18:337–346

33. Hills CE, Bland R, Wheelans DC, Bennett J, Ronco PM, Squires PE (2006) Glucose-evoked alterations in connexin43-mediated cell-to-cell communication in human collecting duct: a possible role in diabetic nephropathy. Am J Physiol Renal Physiol 291: F1045–F1051

34. Tian YC, Fraser D, Attisano L, Phillips AO (2003) TGF-beta1-mediated alterations of renal proximal tubular epithelial cell phenotype. Am J Physiol Renal Physiol 285:F130–F142

35. Hills CE, Willars GB, Brunskill NJ (2010) Proinsulin C-peptide antagonizes the profibrotic effects of TGF-beta1 via up-regulation of retinoic acid and HGF-related signaling pathways. Mol Endocrinol 24:822–831

36. Tian YC, Phillips AO (2002) Interaction between the transforming growth factor-β type II receptor/Smad pathway and β-catenin during transforming growth factor-β1-mediated adherens junction disassembly. Am J Pathol 160:1619–1628

37. Maeda M, Johnson K, Wheelock MJ (2005) Cadherin switching: essential for behavioural but not morphological changes during an epithelium-to-mesenchyme transition. J Cell Sci 118:873–887

38. Strutz F, Zeisberg M (2006) Renal fibroblasts and myofibroblasts in chronic kidney disease. J Am Soc Nephrol 17:2992–2998

39. Humphreys BD, Lin SL, Kobayashi A et al (2010) Fate tracing reveals the pericyte and not epithelial origin of myofibroblasts in kidney fibrosis. Am J Pathol 176:85–97

40. Keeley EC, Mehrad B, Strieter RM (2010) Fibrocytes: bringing new insights into mechanisms of inflammation and fibrosis. Int J Biochem Cell Biol 42:535–542

41. Zeisberg M, Duffield JS (2010) Resolved: EMT produces fibroblasts in the kidney. J Am Soc Nephrol 21:1247–1253

42. Hills CE, Squires PE (2011) The role of TGF-β and epithelial-to mesenchymal transition in diabetic nephropathy. Cytokine Growth Factor Rev 22:131–139

43. Dennler S, Itoh S, Vivien D, Dijke P, Huet S, Gauthier J (1998) Direct binding of smad3 and smad4 to critical TGF-β inducible elements in the promoter of the human plasminogen activator inhibitor-type 1 gene. EMBO 17:3091–3100

44. Yang F, Huang XR, Chung AC, Hou CC, Lai KN, Lan HY (2010) Essential role for Smad3 in angiotensin II-induced tubular epithelial-mesenchymal transition. J Pathol 221:390–401

45. Yeh YC, Wei WC, Wang YK, Lin SC, Sung JM, Tang MJ (2010) Transforming growth factor-β1 induces Smad3-dependent β1 integrin gene expression in epithelial-to-mesenchymal transition during chronic tubulointerstitial fibrosis. Am J Pathol 177:1743–1754

46. Brown KA, Pietenpol JA, Moses HL (2007) A tale of two proteins: differential roles and regulation of Smad2 and Smad3 in TGF-beta signaling. J Cell Biochem 101:9–33

47. Tan R, Zhang J, Tan X, Zhang X, Yang J, Liu Y (2006) Down-regulation of SnoN expression in obstructive nephropathy is mediated by an enhanced ubiquitin-dependent degradation. J Am Soc Nephrol 17:2781–2791

48. Li JH, Zhu HJ, Huang XR, Lai KN, Johnson RJ, Lan HY (2002) Smad7 inhibits fibrotic effect of TGF-Beta on renal tubular epithelial cells by blocking Smad2 activation. J Am Soc Nephrol 13:1464–1472

49. Takenaka T, Inoue T, Okada H et al (2011) Altered gap junctional communication and renal haemodynamics in Zucker fatty rat model of type 2 diabetes. Diabetologia 54:2192–2201

50. Liu L, Hu X, Cai GY et al (2011) High glucose-induced hypertrophy of mesangial cells is reversed by connexin43 over-expression via PTEN/ Akt/mTOR signaling. Nephrol Dial Transplant. doi:10.1093/ndt/gfr265